Materials Science & Engineering C 118 (2021) 111369

Contents lists available at ScienceDirect

Materials Science & Engineering C

journal homepage: www.elsevier.com/locate/msec

Channeled polysaccharide-based hydrogel reveals influence of curvature to guide endothelial cell arrangement in vessel-like structures

Teresa Simon-Yarza*, Marie-Noëlle Labour, Rachida Aid, Didier Letourneur

INSERM U1148, Universié de Paris, Université Sorbonne Paris Nord, X Bichat Hospital, 46 rue H. Huchard, 75018 Paris, France

ARTICLE INFO

Keywords:
Hydrogels
Microarchitecture
Structured material
Tissue engineering
Vascularization

ABSTRACT

Within the biomaterials proposed for tissue regeneration, synthetic 3D hydrogels that mimic soft tissues possess great potential for regenerative medicine but their poor vascularization rate is usually incompatible with long-term cell survival. Fabrication of biomaterials that promote and/or accelerate vascularization remains nowadays a challenge. In the present work, hydrogels with tubular geometries ranging from 28 to 680 μm in diameter, that correspond to those of human small artery/veins and arterioles and venules, were prepared. The surface of this tubes was coated with proteins of the extracellular matrix assuring the adhesion of endothelial cells in a monolayer. Interestingly, in the case of small diameter channels, polysaccharide-based hydrogels made of neutral pullulan and dextran that do not allow endothelial cell adhesion, were transformed into active materials guiding endothelial cell behavior solely by modification of the internal microarchitecture, without addition of proteins. Under static conditions, endothelial cell adhesion, migration, proliferation and polarization on the hydrogel was induced, without the addition of any extracellular matrix protein or adhesion peptide; this property was found to be directly dependent on the curvature of the internal channels. In the last years, the impact of the geometry of biomaterials to regulate cell behavior has been highlighted paving the way to use non-flat geometries as cues to develop biomaterials to guide tissue regeneration. Here, we report a functional material based on geometrical cues to assure endothelial cell arrangement in tubular vessel-like structures and providing with new pro-vascularizing properties.

1. Introduction

Hydrogels are proposed for tissue regeneration due to their high content in water and soft consistency that mimic those of the tissues [1,2]. Hydrogels are versatile biomaterials used to treat a wide variety of tissues [3]. In the case of tissue engineering, their similarities with the extracellular matrix (ECM) make of them the most suitable materials for tissue regeneration. Polysaccharides are widely used in tissue engineering. Polysaccharides, along with proteins, are the essential components of the ECM. For some years, dextran and pullulan have demonstrated their suitability in tissue engineering with different cell types. Our team has carried out several studies that reveal the versatility of hydrogels prepared from pullulan and dextran, based on the possibility of controlling their properties such as geometry, mechanical properties and porosity [4–6]. Nevertheless, poor vascularization rate of hydrogels is often incompatible with long-term cell survival. This is due to the lack of oxygen and nutrient supply resulting from the lack of blood vessels in the material. That is why vascularization of biomaterials that can interact with the host vasculature to form anastomosis is currently in the spotlight of tissue engineering and regenerative medicine [7,8]. In this context, a major challenge is the formulation of materials that stimulate angiogenesis and blood vessel formation.

Angiogenesis is a complex process usually initiated by a hypoxic stimulus in the tissue [9]. As a result, a quiescent vessel is activated leading to vessel sprouting. Matrix metalloproteinases act degrading the ECM and endothelial cells (EC) are able to migrate onto this ECM in a well-orchestrated way following integrin signaling. Sprouting is leaded by one endothelial cell, the tip cell, characterized by the lamellipodia and filopodia in their cytoskeleton, followed by stalk cells that are found between the quiescent cells and the tip cell, and that are the ones to proliferate to constitute the new endothelium. This angiogenic process is partially modulated by the ECM that is known to provide physical scaffolding to the cells, together with biochemical and biomechanical cues that assure structural integrity of the tissues as well as tissue morphogenesis and regeneration [1,10]. Numerous materials have been proposed to be functionalized with pro-angiogenic factors and motifs following a biomolecule-based approach to promote vessel formation [11–14]. Many of these works are based on the delivery of

* Corresponding author.
E-mail address: teresa.simon-yarza@inserm.fr (T. Simon-Yarza).

https://doi.org/10.1016/j.msec.2020.111369
Received 20 March 2020; Received in revised form 27 July 2020; Accepted 5 August 2020
Available online 11 August 2020
0928-4931/

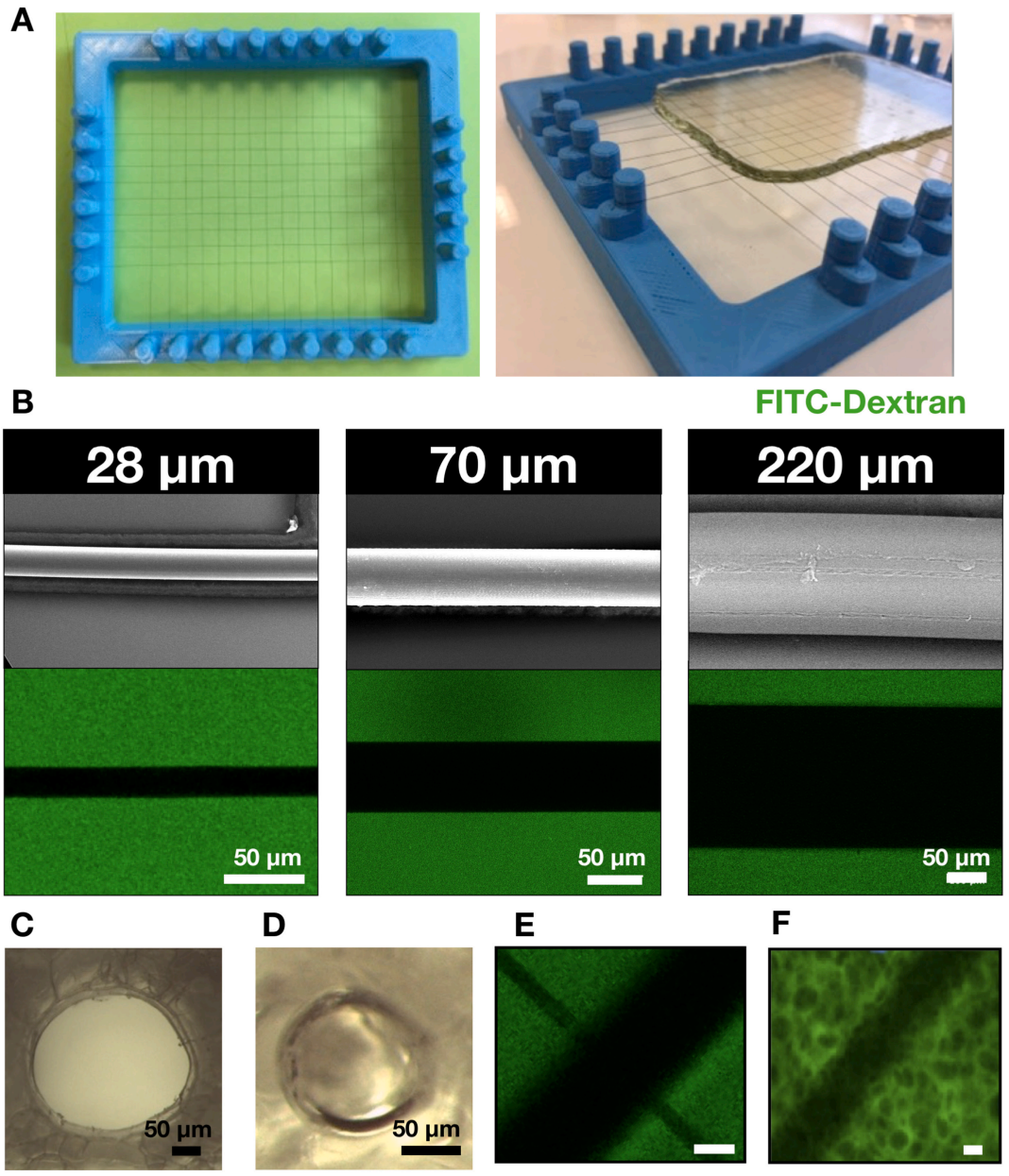

Fig. 1. Polysaccharide-based hydrogel internal geometry was modified during cross-linking. A) A 3D printed mold was used to incorporate clinical-grade polyamide-6 filaments during cross-linking of the polysaccharides (left), and the hydrogel was formed around the filaments (right). B) SEM images of the filaments of 28, 70 and 220 µm in diameter demonstrated smooth surfaces that led, after removal of the filaments, to the formation within the fluorescent hydrogels of channels without any patterning that could affect cell behavior. C) The shape of channels remained after freeze-drying and D) rehydration in 0.9% NaCl, that modulated channel diameter (see scale bars in C and D). E) This approach allowed the formation of crossing channels of different diameters and F) combining pores and channels within the same hydrogel after freeze-drying. Scale bar: 50 µm.

pro-angiogenic growth factors to promote vascularization *in vivo* [11–14]. More recently, material vascularization has been proposed based on the *in vitro* formation of microvessels within 3D materials that present pre-formed channels in their structure, prior to implantation [16–23]. Different strategies to form these channels have been described, such as the use of syringes [16], glass micropipettes [16], half circular molds [17,18] or sacrificial structures made of soluble materials [15,19–21] or photodegradable gels [22,23]. To assure cell adhesion, they include in their composition molecules that mediate cell adhesion: RGDS sequences [22] and proteins of the ECM [11–15,21], such as collagen, fibrin or fibronectin. A limitation to transfer this strategy to the clinic is their high cost as well as the immunogenic potential of these biomolecules. Besides, any of these materials presented pores in its structure to locate other cell types to perform co-culture; only in some cases a second cell type was encapsulated in the fibrin or matrigel hydrogel [19,22]. For further information, the latest works dealing with the engineering of hydrogels with perfusable microchannels were recently reviewed elsewhere [21].

All things considered, the ideal biomaterial to favor endothelialization for tissue engineering and regenerative medicine applications should fulfill the following requirements: 1) present interconnected hollow channels of a wide range of diameters similar to those of vessels, 2) promote endothelial cell arrangement in monolayers leading to microvessel-like structures, 3) allow co-culture of other cells in “physiological” conditions, 4) biocompatible composition (pharma grade materials), 5) easy to fabricate, 6) cost-efficient. Ideally, the material should be able not only to assure cell adhesion on the walls of the hollow channels, but also to induce pro-angiogenic endothelial cell

behavior.

This work introduces a different and innovative biomolecule-free approach to confer neovascularization functions to materials based on geometry. In the last years, the impact of materials geometry to regulate cell behavior has been highlighted. Recent works have demonstrated that functional materials can be prepared by including geometric features to modify cell migration and differentiation, paving the path to use non-flat geometries as cues to develop biomaterials to guide tissue regeneration [10,24–34]. Nevertheless, the knowledge of how cell behavior is influenced by non-flat geometries is still limited and poorly applied in the material science to modify the properties of a biomaterial to improve its regenerative potential. This is in part due to the limitations to manufacture bioinert materials with smooth channels with a wide range of diameters to perform *in vitro* studies.

In this study, an innovative and simple fabrication method to form hollow tubular structures within a hydrogel scaffold compatible with cell culture and made of neutral polysaccharides is described (Fig. S1). Based on the results obtained with this tool, we report the first work in which modification of the geometry of a hydrogel solely drastically changed cell-material interactions assuring endothelial cell arrangement in tubular capillary-like structures and provided new pro-angiogenic properties. From now on, we will refer to these channeled hydrogels as non-flat hydrogels to emphasize the difference between a flat 2D surface (x,y) and a tubular or channeled geometry in the three axes (x,y,z).

2. Experimental

2.1. Hydrogel preparation and characterization

2.1.1. Polysaccharide cross-linking

Pullulan (Mw 200 kDa; Hayashibara Inc.) and dextran (Mw 500 kDa; Pharmacosmos) at a 3:1 ratio were mixed to prepare a 0.3 g/mL polysaccharide solution. After activation of hydroxyl group with NaOH 10 M solution, crosslinker sodium trimetaphosphate (STMP) was added and the whole was poured into the mold and incubated at 50 °C during 20 min. Three concentrations of STMP were used: 1.5%, 3% and 5%, equivalent to 12.5 mg/g polysaccharide, 25 mg/g polysaccharide and 41.6 mg/g polysaccharide respectively. Except when indicated, the hydrogels used in the study correspond to the 3% STMP solution. Hydrogel was rinsed in PBS 10 X once, for fast pH neutralization, and then in milli-Q water to remove salts until ionic force of the rinsing water was found below 20 μS (Conductivity Meter Thermo Orion model 145). For confocal observation, 10 mg FITC-Dextran (Mw 500, TdB Consultancy) were added to the polysaccharide solution. Agarose gels were prepared by diluting different amounts of agarose (Invitrogen Life Technologies) (0.7–2.5% w/v) in hot water (40 °C). Hydrogels were prepared by pouring the polysaccharide solution within 2 glass plates separated by a 1 mm spacer. After rinsing, the gel was cut into discs (5 mm diameter). 2D Hydrogels for cell adhesion evaluation were directly poured on 12-well plate dish (Corning®).

2.1.2. Micro-channel and pore formation

To form micro-channels, hydrogels were casted using a mold in which clinical-grade polyamide-6 filaments (Ethicon) were included (Fig. 1). This mold made of poly-lactic acid was conceived by Fusion 360 Autodesk software and 3D printed using an Ultimaker Original + printer.

Pores were obtained with a freeze-drying protocol. Hydrogels were embedded in PBS: water (1:6) salt solution and transferred to the freeze dryer (Cryotec). Controlled freezing phase of the samples at −20 °C was followed by a sublimation phase under controlled low pressure with an increase of temperature. For specific coating of the channels, samples were incubated for 2 h at room temperature in a collagen type I from rat tail solution (BD-#354236) (0.5 mg/mL^{-1}) in 0.01 N HCl. Collagen fiber deposition on the channels was done by pH neutralization through incubation in PBS: water (1:6) at pH 7.4 prior to freeze drying and pore formation. Freeze-drying led to sponge-like scaffolds that were stored at room temperature until their rehydration, to be characterized and employed for cell seeding as hydrogels.

2.1.3. Channel diameter measurement

Hydrogels containing FITC-Dextran and channels with different diameters were immersed in water, PBS or culture media. Media were exchanged until the ionic force remained constant (Conductivity Meter Thermo Orion model 145). Then, confocal microscopy of hydrated samples was used and image acquisition was done with a confocal microscope LSM 510 Zeiss and optical sections comprising the whole channel were collected with a step-size of 5 μm. Images were acquired with ZEN lite software and image analysis was done with ImageJ software. Channel diameter in different media was established measuring the maximal distance between channel walls. Analysis was done in triplicate.

2.1.4. Hydrogel equilibrium water content

To calculate equilibrium water content, a gravimetric method was followed. Samples (5 mm diameter, 1 mm thickness; n = 3) were dried by freeze-drying (Cryotec), weighted (W0) and then immersed in excessive distilled water overnight at room temperature. Swelling equilibrium of hydrated samples was reached when samples weight remained constant (W1). Then, % of water content was calculated using the formula: $((W1 - W0) / W1) \times 100$.

2.1.5. SEM imaging

The topography of clinical-grade polyamide-6 filaments was observed using a Scanning Electron Microscope (JEOL JSM-IT100, software InTouch Scope Version 1.060) under low vacuum conditions.

2.1.6. Elastic modulus

The elastic moduli of the hydrogels were measured in the linear viscoelastic region using a Discovery HR-3 Hybrid Rheometer. Disk-shaped samples (40 mm diameter, 1 mm thickness) were analyzed using the following parameters: 0.5 N force, 0.25% strain and 0.05–5 Hz frequency range. Analysis was done in triplicate.

2.1.7. Collagen coating assessment

To confirm collagen coating in the micro-channels of non-porous and porous hydrogels, two methods were followed. First, hydrogels were stained using picrosirius red dye that binds collagen. After 2 h incubation at room temperature, hydrogels were extensively washed with PBS until complete removal of the unbinded dye (this was confirmed by using hydrogels without collagen as controls). Then, confocal microscopy was employed based on the fluorescence emitted by collagen fibers after picrosirius red staining. Confocal microscope LSM 510 Zeiss was used and images were acquired with ZEN lite software and image analysis was done with ImageJ software.

2.2. In vitro studies

2.2.1. Cell culture inside the hydrogel

Three different cell types were used in the *in vitro* studies, namely human umbilical endothelial cells (HUVEC) (ATCC CRL-1730), fibroblasts NIH3T3 or hepatic carcinoma HepG2. HUVEC cells were cultured in T75 surface treated flasks (Corning®) in endothelial cell medium following the provider recommendations. HepG2 and NIH3T3, were also cultured in T75 surface treated flasks using a DMEM (4.5 g/L glucose) supplemented with 10% fetal bovine serum and 1% antibiotic/antimycotic solution (all purchased by GIBCO). Cells were splitted according to manufacturer and kept in an incubator prior to use (37 °C, 5% CO_2).

Cell seeding was done with a syringe-induced vacuum method to introduce human umbilical endothelial cells, fibroblasts NIH3T3 or

hepatic carcinoma HepG2 cells in the channel. First, cells were detached with 1 mL Trypsin solution (Gibco) at 37 °C for 5 min; trypsin was inactivated by performing cell dispersion in complete cell medium and then centrifuged and counted. Cell dilution in complete cell culture medium was done to reach the desired concentration. To load the cells in the channels, hydrogels and cell suspension were introduced in a 10 mL syringe barrel. A 3-way stopcock was used to close the system and the plunger was pulled to make cell suspension circulate inside the channels. Then, cell-loaded hydrogels were placed in a 24 well-plate, complete cell medium was added and plates were placed in an incubator. For the adhesion studies with collagen type I from rat tail (BD-#354236), hydrogels were incubated for 2 h at room temperature in a 2 mg/mL collagen acid solution and rinsed with excess of PBS to cause collagen fiber precipitation prior to cell culture. Except where indicated, cell seeding was done at a concentration of 5,000 cells/μL.

Cell culture on 2D hydrogels was done by pouring cell suspension, 100,000 cells/well, on 12-well plate dish pre-coated with the hydrogel.

2.2.2. Cell metabolic activity

Cell metabolic activity was quantified using a Resazurin assay (Sigma R-6892). Briefly, cells were cultured on 12-well plate dish coated or not with PUD hydrogel. After 24 h, cell medium was removed and fresh culture medium containing 10% resazurin solution was added. 2 h later, 100 μL of medium were transferred to a 96-well plate and fluorescence was measured at a wavelength of 590 nm using an excitation wavelength of 560 nm. Analysis was done in triplicate.

2.2.3. Cell seeding efficacy

Immediately after cell seeding, optical microscopy was used to count the number of cells inside the channels (N). Seeding efficacy was calculated considering the volume inside the channels and amount of cells in the same volume of the cell suspension (Ns), taking into account cell concentration. Then, efficacy was calculated in percentage as follows: N/Ns × 100. Analysis was performed in at least 12 samples per group of study.

2.2.4. Cell staining and confocal imaging

Actin filaments were labeled by incubation with Alexa-Fluor 647 Phalloidin (Invitrogen) (1/200, 1 h incubation time at room temperature) after fixation in paraformaldehyde 4%. Laminin was stained using rabbit polyclonal antibody (ab19012) (1/400, overnight incubation at 4 °C) followed by secondary antibody Alexa-Fluor 647 anti-rabbit (ab150079) (1/500, 2 h incubation time at room temperature). Nuclei were stained with DAPI (1/50,000).

Image acquisition was done with a confocal microscope LSM 510 Zeiss. Images were acquired with ZEN lite software and image analysis was done with ImageJ software.

2.2.5. Cell density quantification within the channels

Number of cells/mm^2 within the channels was quantified using ImageJ software. At different times after cell seeding, samples were fixed and actin filaments and DNA stained as previously described. Samples were observed and images were acquired by confocal microscopy. Cell density was calculated normalizing the number of nuclei per channel area. The ratio of adhered and non-adhered cells was also estimated by this method. Analysis was done in triplicate.

2.3. Statistical analysis

Non parametric Mann-Whitney test was used to compare unpaired samples.

3. Results

3.1. Hydrogel preparation and characterization

Chemical cross-linking of pullulan and dextran using STMP as cross-linking agent led to the formation of transparent hydrogels with high water retention capacity (> 92% water at equilibrium) (Fig. 1A). The mechanism of cross-linking of pullulan with STMP was proposed in 2004 by Mocanu et al. [35] In brief, after polysaccharide activation in the presence of NaOH, both polysaccharide and NaOH react with STMP causing ring-opening and the apparition of grafted sodium tripolyphosphate (gSTPP) and the degradation product STPP, respectively. Then, gSTPP reacts with phosphate groups leading to the formation of three species: the crosslinked chain, the grafted chain and inorganic pyrophosphate [36]. Performing cross-linking around polyamide-6 filaments led to permanent modifications of the microarchitecture of the hydrogel, that presented micro-channels of different diameters ranging from 28 μm (curvature κ = 1/14) to 680 μm (curvature κ = 1/390) (Fig. 1A and B). The smoothness of the polyamide-6 filaments was confirmed by SEM prior to channel formation (Fig. 1B). Micro-channels remained well formed even after freeze-drying (Fig. 1C) and re-hydration (Fig. 1D), which caused a decrease in the diameter of the channel due to the swelling of the material. Using this method it was possible to combine filaments with different diameters in the same hydrogel and to form interconnected micro-channels of several diameters (Fig. 1E). In the case of freeze dried hydrogels, channels were surrounded by pores formed by water crystal formation and sublimation (Fig. 1F). Mechanism of pore formation and freeze-drying parameters determining porosity in the hydrogels have been recently described by some of us elsewhere [4]. Channel coating with collagen was confirmed by picrosirius red staining and fluorescent microscopy (Fig. S2). A second freeze-drying cycle, following collagen coating, made possible to specifically coat micro-channels without modifying the surface of the pores and assuring cell adhesion exclusively in the channel. This is particularly interesting for further applications, such as co-culture of non-adhesive cells or organoids within the pores surrounded by endothelialized channels. Channel formation method was also used to successfully modify the architecture of hydrogels with a different composition such as agarose (Fig. 2).

Of note, swelling of the PUD hydrogel was dependent on the ionic strength of the hydrating solution: the higher the ionic force, the less the hydrogel swelling. This impacted also the diameter of the micro-channels as shown if Fig. 3A. Indeed, when the same hydrogel prepared with a filament of 70 μm was immersed until equilibrium in water (5 μS), PBS (10 mS) or cell culture medium (11 mS), micro-channel diameter in the hydrogel varied from 127 μm, to 115 μm and 100 μm respectively. In the case of PUD hydrogels, swelling capacity of the material was also related to the cross-linking ratio (Fig. 3B). As the feeding ratio of STMP increases, the final diameter obtained with the same filament was reduced (117 μm for 1.5% STMP; 113 μm for 2% STMP; 98 μm for 3% STMP; 95 μm for 4% STMP; 90 μm for 5% STMP). Increased cross-linking also caused an increase of the elastic modulus (from 300 Pa to 3 kPa corresponding to 1.5% STMP and 5% STMP respectively) (Fig. S3).

3.2. In vitro endothelial cell studies

3.2.1. In vitro studies

Cells seeded on 2D hydrogels did not adhere to the polysaccharide matrix (Fig. 4A). After 1 h, individual cells presented a spherical non adhesive phenotype, and after 24 h, cell aggregates were founded on the surface of the hydrogel. Lack of adhesion was confirmed since cells slided off during hydrogel manipulation and were not found on the surface of the material after 72 h.

Endothelial cells were cultured inside the channels under static conditions and standard media without any additional biochemical

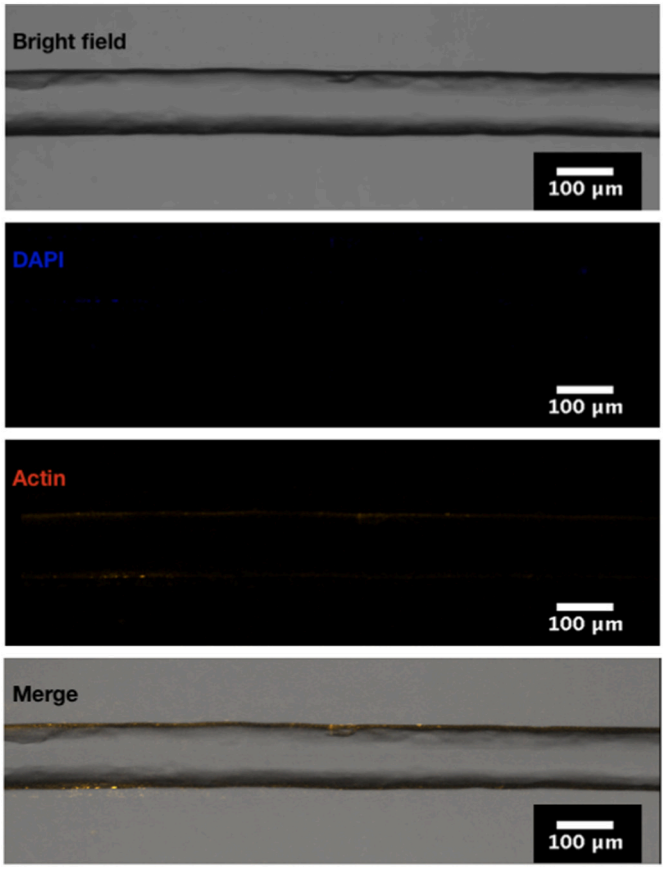

Fig. 2. Agarose tubular hydrogels. One week after endothelial cell seeding in agarose gels fabricated with tubular constructs, no cell adhesion or cell aggregates in the lumen were observed. From top to bottom: bright field channel, split blue channel for DAPI, split red channel for Actin, and merge channel. (For interpretation of the references to color in this figure legend, the reader is referred to the web version of this article.)

supplementation. The optimal number of cells to seed in the channels was tested with 2500, 5000 and 10,000 cells/µL. In all cases, the efficiency of cell seeding was similar with 44%, 58% and 45%, for 2500, 5000 and 10,000 cells/µL, respectively. The number of cells present in the channel immediately after seeding, was 27.8 ± 15, 72.5 ± 27, and 111.3 ± 60 cells for 2500, 5000 and 10,000 cells/µL, respectively. Cell adhesion was already observed after 6 h in channels with a diameter below or equal to 100 µm (curvature $\kappa = 1/50$ µm-1), which is about 10 times the size of endothelial cells in a non-spread state. Condition with 2500 cells/µL showed low cell coverage and 5000 cells/µL led to a higher variability compared to 10,000 cells/µL. Therefore, we choose 5000 cells/µL as working concentration for further experiments. Using these conditions, cell metabolic activity within the microchannel was quantified showing an increase after 96 h that became significatively more important after 164 h (Fig. 4B).

The same experiment was performed in hydrogels presenting larger diameter (> 100 µm). In this case results were completely different: cells progressively formed small aggregates inside these channels, regardless of cell concentration (Fig. 5). After one week, few cells survived in large channels and only a few adhered on the walls in a highly heterogeneous way (Figs. 5A and S4). HepG2 cells and NIH3T3 behaved similarly to HUVEC in large diameters, with the difference that no cell adhesion was observed, regardless of the diameter of the channel.

In the case of hydrogels incubated with collagen type I (2 mg/mL) prior to cell seeding, cell adhesion occurred within the first hours after cell seeding even in larger channels (Fig. S4).

3.2.2. *Micro-channel cell lining with endothelial cells*

Following the curvature-dependent spontaneous adhesion of endothelial cells in the small channels of hydrogels, that did not occur on 2D hydrogel (Fig. 4A), cell behavior with time was further studied (Fig. 6). The number of cells found in the channels (Fig. 4B) significantly increased with time. The percentage of cells in a spread state was also significantly higher at 48 h (72%) compared to 24 h (2%). Regarding cell morphology, a peculiar cell organization was detected from the beginning and adhered cells aligned following the long axis of the channel already after 24 h (Fig. 6A).

In the following hours after adhesion, cells continued to proliferate from the bottom of the channels forming a monolayer of cells, whereas few cells got polarized on the sides of the walls. At 48–72 h, three different cell morphologies were clearly identified (Fig. 6B): a) spread cells with central nucleus forming a monolayer (Fig. 6B insert in the right), b) polarized cells with actin assembled in lamellipodia and filopodia (Fig. 6B left and right highlighted with symbol ✚), and c) aligned cells (Fig. 6B right highlighted with symbol ✪) that were located between (a) cells at the bottom of the channel and (b) polarized cells at the top of the channel.

To assure full cell lining of channels, we turned 180° the hydrogel twice following the protocol described in Fig. S5. This way, after only 7 days, we could fabricate *in vitro* 5 mm-long capillary-like cell tubes with < 100 µm diameter and full cell coverage (Fig. 7A&B). Within these newly formed capillary-like structures, the presence of ECM proteins present in the natural basal membrane of the endothelium, such as laminin, was observed by immunofluorescence (Fig. 7C), as well as focal adhesions in the cell membranes (Fig. 7D).

4. Discussion

Pullulan/dextran hydrogels were prepared by cross-linking with sodium trimetaphosphate in water as previously described [37]. Hydroxyl groups in the polysaccharides are activated at basic pH, and hydroxyl groups of polysaccharides react with cyclic STMP that opens and cross-links, leading to hydrogel formation [45]. These biocompatible hydrogels have been already demonstrated as interesting scaffolds

A

Filament diameter	Channel diameter in water (≈5 µS)	Channel diameter in PBS (≈10 mS)	Channel diameter in culture medium (≈11 mS)
28 µm	39 µm	38 µm	35 µm
70 µm	127 µm	115 µm	100 µm
220 µm	390 µm	312 µm	300 µm

B

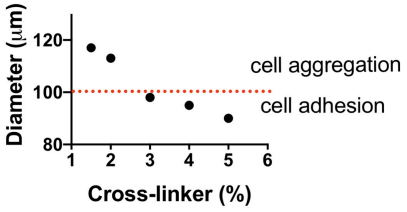

Fig. 3. Channel diameter varied with both the cross-linker content and the ionic strength of the swelling solution. A) An inverse correlation was observed between channel diameter and the ionic strength of the swelling solution. B) Channel diameter decreased with the increase of cross-linker % introduced during hydrogel formation and the resulting hydrogel induced cell adhesion or cell aggregation.

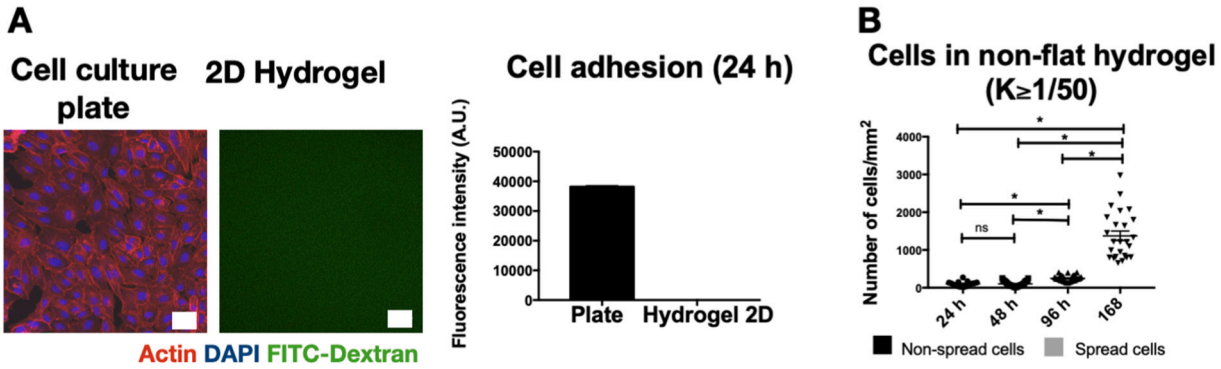

Fig. 4. Endothelial cell behavior in 2D hydrogels *vs.* non-flat hydrogels with channels with a curvature over 1/50 μm. A: cells adhered on cell culture flasks but did not adhere on the surface of 2D hydrogels (left) where any cell metabolic activity could be detected by Resazurin assay after 24 h (right). Scale bar: 50 μm. B: in channels with a curvature over 1/50 μm, cells spontaneously adhered and proliferated (* = $p < .0001$).

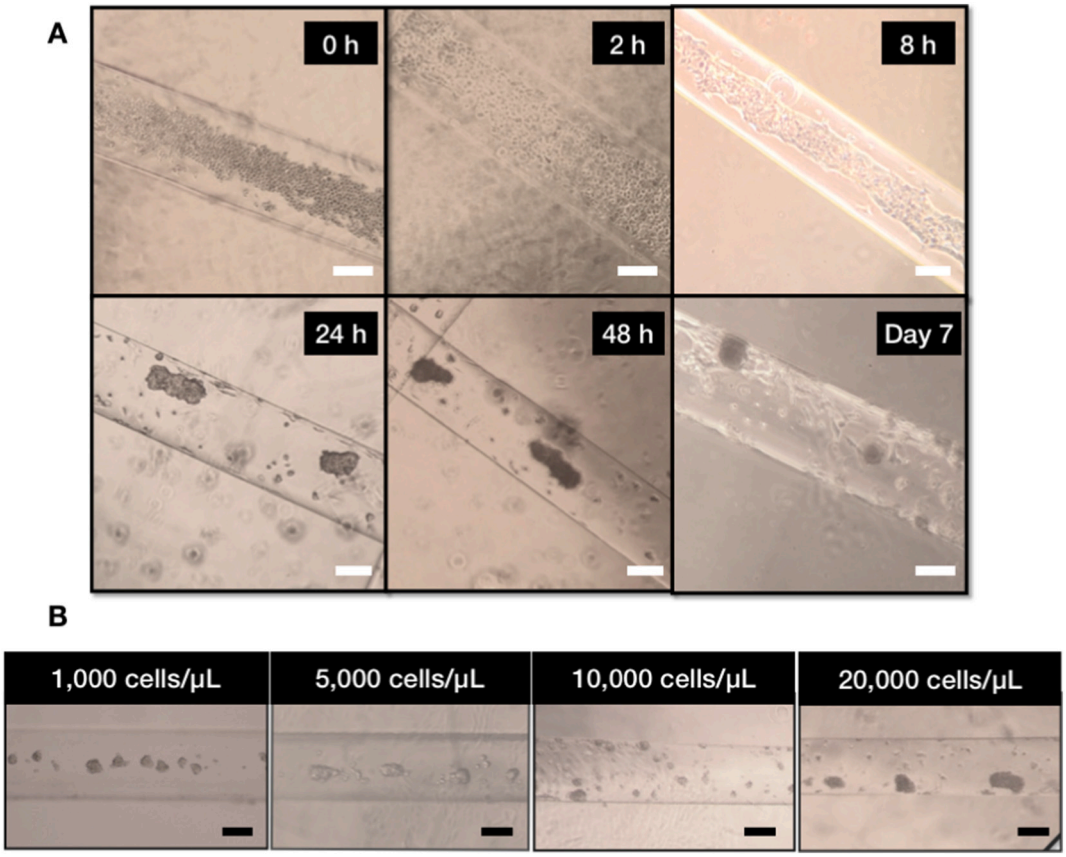

Fig. 5. Formation of cell aggregates in channels with a diameter > 100 μm. A: Kinetics of aggregates formation from Day 0, immediately after cell seeding (5000 cells/μL) to Day 7. At Day 7, some cells adhere to the hydrogel likely due to the secretion of ECM by the cells. B: Aggregate formation in channels with a diameter > 100 μm was independent of cell density: the images show aggregates in the channels 24 h after cell seeding with cell suspensions from 1000 to 20,000 cells/μL. Scale bar: 100 μm.

for 3D cell culture, cell therapy and tissue engineering approaches [5,37–39]. Due to the high content in water (> 92%) and the chemical structures of the polysaccharides, endothelial cells do not adhere spontaneously to these materials [37,38], as shown in Figs. 4A and 8A. Here, using only these neutral polysaccharides, microarchitecture was simply created during the cross-linking process and micro-channels of different diameters ranging from 28 μm (curvature κ = 1/14 μm) to 680 μm (curvature κ = 1/390) were formed within the hydrogel (Fig. 1).

To study the role of non-flat geometry on cell adhesion and cell behavior, polysaccharide-based hydrogels without addition of ECM proteins or growth factors were employed. The hydrogel was cross-linked around clinical-grade filaments with different diameters that determined the final diameter of the micro-channels (Fig. 2A). The use of clinical-grade filaments to form channels in materials presents numerous advantages compare to other developed strategies. Clinical-grade filaments are clinical approved, sterile and commercially available in a wide variety of well-defined diameters (from 20 μm to 900 μm) and compositions, being non-degradable or degradable. Degradable filaments are interesting to be used as sacrificial tubular structures.

To assure the formation of smooth channels without any micro-pattern that could affect cell behavior, the smooth surface of filaments was confirmed by scanning electron microscopy (Fig. 1B). Once the

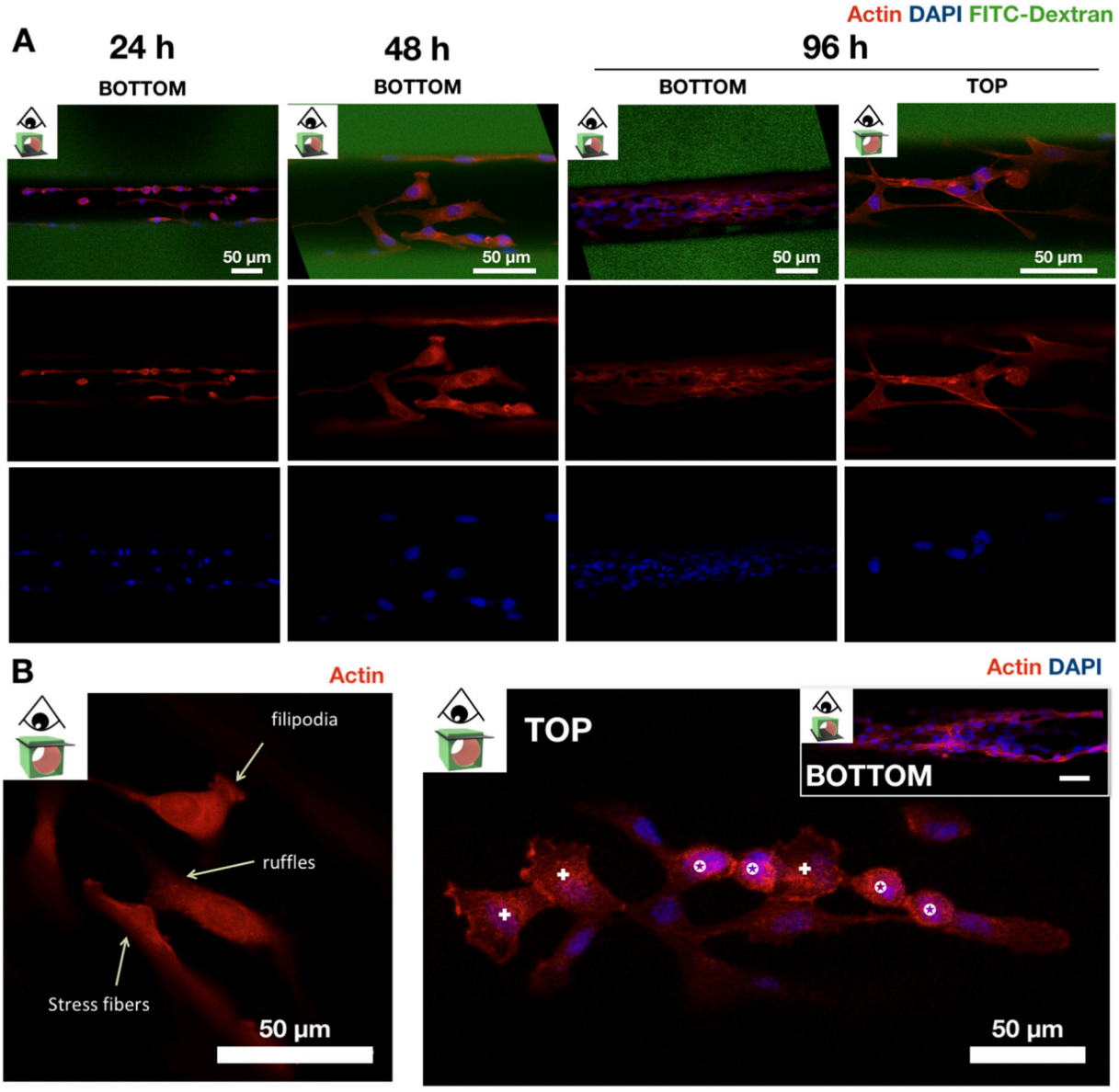

Fig. 6. Endothelial cell behavior in non-flat hydrogels with channels with a curvature over 1/50 µm. A) Cell alignment spontaneously occurred during the first 24 h (first row), followed by cell migration characterized by the presence of polarized cells highly visible at 48 h (second row), and proliferation. At the bottom of the channels, cells formed after 96 h a continuous layer of cells (third row), whereas at the top, they were still organizing networks rather than full layers (fourth row) (from top to bottom: merge channel, split red channel for Actin, and split blue channel for DAPI). B: At 48–72 h, three different endothelial cell morphologies co-existed: i) migrating cells presenting filopodia in their structure (left and right: cells highlighted with symbol ✚) as well as ii) not-migrating cells, with a central nucleus (right: cells highlighted with symbol ✪) that were found between the migrating cells and iii) the cells at the bottom forming a full monolayer (right: insert). Scale bar: 50 µm. (For interpretation of the references to color in this figure legend, the reader is referred to the web version of this article.)

polysaccharides were cross-linked, hydrogels were incubated in PBS to neutralize pH and to swell so that the filaments could be easily removed without damaging the structure. Of note, the use of degradable filaments such as PLA and a short incubation in acidic conditions could avoid this step, or could be also obtained later on *in situ* after implantation. Micro-channels remained well formed even after freeze-drying (Fig. 1C) and re-hydration (Fig. 1D) demonstrating that this process is an easy way to permanently modify the internal architecture of porous and non-porous hydrogels. The obtained hydrogels were transparent making possible the direct observation of cells inside the channels by conventional bright field microscopy (Fig. 5). Moreover, the versatility of the casting method was evidenced by the formation of different sizes of channels inside the hydrogels (Fig. 1B) combining filaments with different diameters and also interconnected micro-channels of several diameters (Fig. 1E). This preparation method was also used to successfully modify the architecture of different hydrogels such as agarose gels (Fig. 2).

When compared to other technologies, is worth noting the simplicity of our approach [40]. Unlike laser, stereolitography or bioprinting-assisted techniques, no particular technology is needed. Compared to bioprinting, resolution is better, fabrication is faster, and we overcome limitations related to printability of the biomaterial. Compared to stereolitography, we do not require the presence of photocrosslinkable groups and photoinitiators that have been associated with cell toxicity, and remain a drawback for clinical translation. Other casting methods have been described in several steps, such as in the work of Nie and colleagues, where 5 steps are reported, namely i) printing chips with microgrooves, ii) pouring the solution on the chips, iii) cross-linking, iv) demolding of the hydrogel sheets, v) bonding of two sheets by photo-cross-linking [41,42]. This complex process contrasts with our method

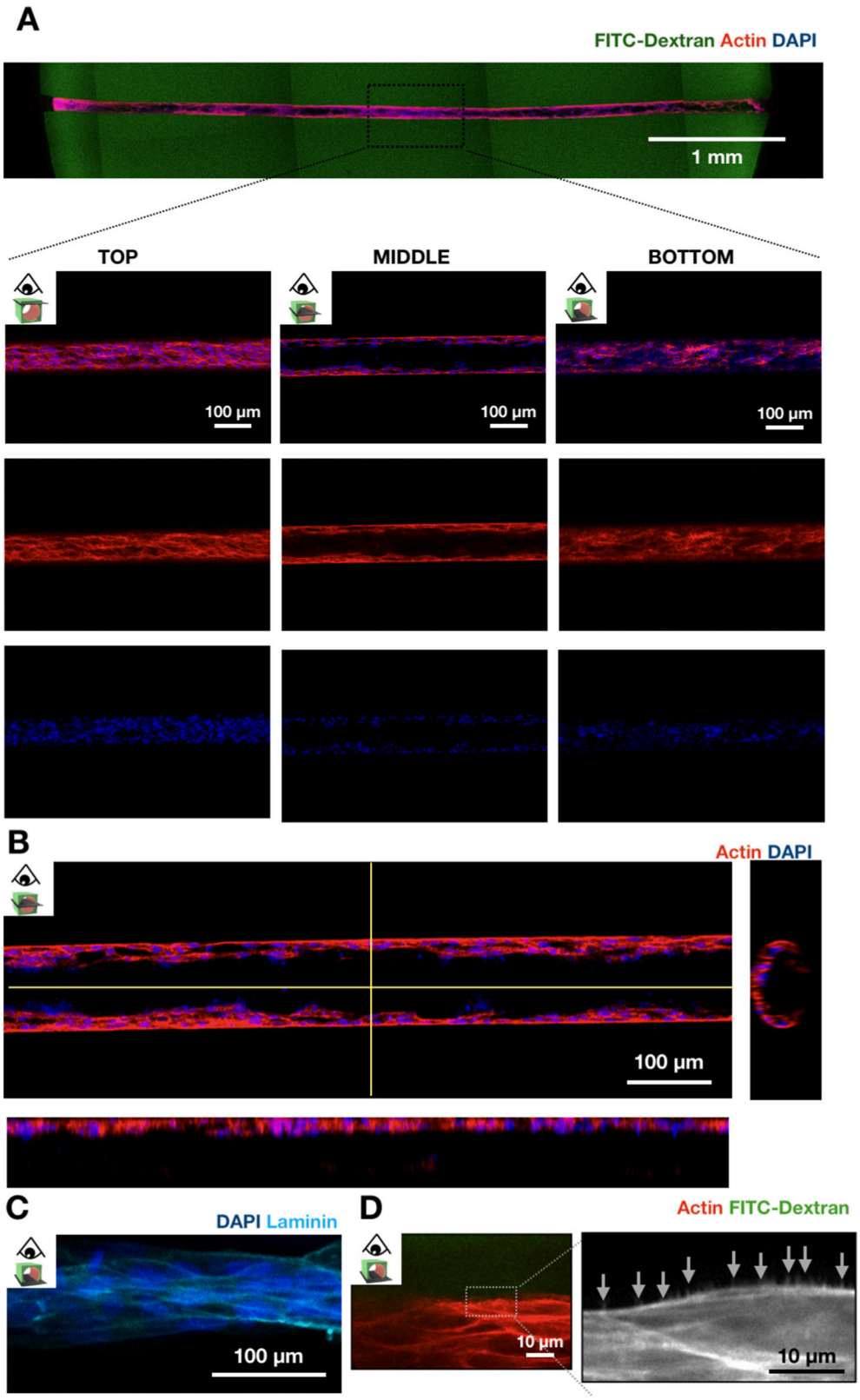

Fig. 7. Geometry guided endothelial cell lining. A) After 7 days under static conditions in regular media without additional ECM proteins or exogenous growth factors, endothelial cells formed capillary-like structures with 5 mm length and 70 µm diameter (upper image) inside the hydrogel (in green). Below, larger magnification using confocal microscopy demonstrated the arrangement of cells in capillary-like structure with the presence of a layer of cells coating the tube and an internal lumen (from left to right in the figure: top, middle and bottom of the channel; from top to bottom: merge channel, split red channel and split blue channel). B) Detail of a section of the capillary-like structure with confocal images with orthogonal views that demonstrated the presence of a monolayer of cells covering the channels. C) Laminin was detected as representative of the secretion of the ECM by endothelial cells. D: cells adhered to this newly formed ECM through focal adhesion sites characterized by actin protrusions (arrows). (For interpretation of the references to color in this figure legend, the reader is referred to the web version of this article.)

where channels are directly formed around the filament in hydrogels composed made of unmodified pharmaceutical-grade polysaccharides from natural origin.

We then investigated the role of internal micro-channels, in particular the role of the curvature on endothelial cell behavior on PUD gels. Cell adhesion in the absence of proteins of the ECM only occurred in the channels with a curvature below 1/50 µm, indicating that cells were able to sense the curvature and respond to it. This difference was observed independently of the number of cells seeded in a wide range of cell concentration (from 1000 to 20,000 cells/µL) (Fig. 5B). Interestingly, the nature of the polysaccharides that constituted the hydrogel was a relevant factor in this geometry-induced adhesion. When

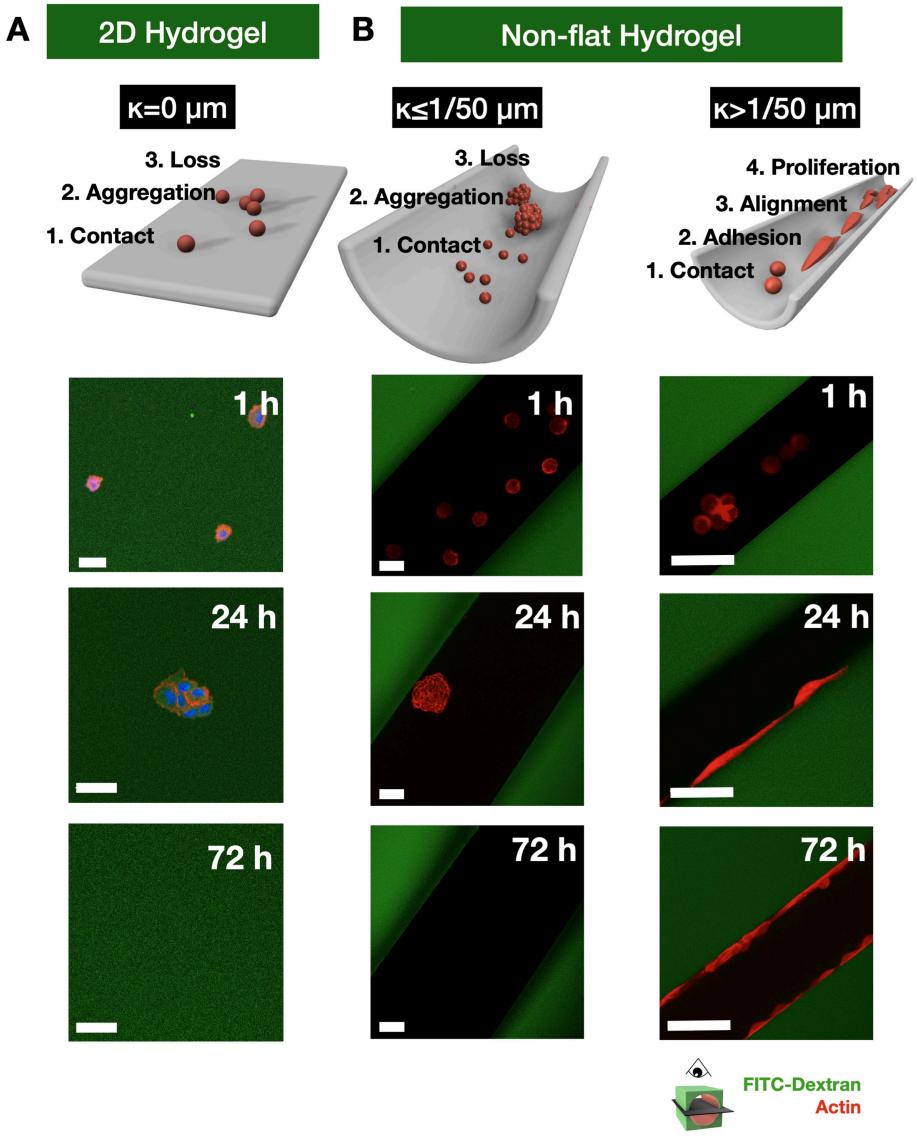

Fig. 8. Endothelial cell behavior depends on material geometry on Pullulan/dextran hydrogel. A: in 2D, cells do not adhere firmly on hydrogels. B: in non-flat hydrogels, cell adhesion on hydrogels is determined by the diameter of the channels: in channels with a curvature below 1/50 μm-1 (B left), equivalent to a diameter > 100 μm, cells behave as on 2D materials; in smaller diameters with a curvature greater than 1/50 μm-1, endothelial cells are able to adhere and to proliferate (B right). Representative confocal images after 1 h, 24 h and 72 h are reported using FITC-Dextran for green label of the hydrogel red staining for actin and blue for nucleus. Scale bars = 50 μm for all panels. (For interpretation of the references to color in this figure legend, the reader is referred to the web version of this article.)

performing the same experiments with agarose gels at low (0.7%) and high (2.5%) concentrations, to assure a broad range of Elastic Moduli, no cell adhesion was observed, regardless the agarose concentrations or channel diameters (Fig. 2). Moreover, these results allow to discard the hypothesis of an effect due to cell confinement or to the flow caused by a phenomenon of capillarity in the small channels compared to the large ones. Besides, lack of cell adhesion and aggregate formation was also observed when other adherent cell types, namely fibroblast 3T3 and hepatic carcinoma cell line HepG2, were seeded in the PUD microchannels. This indicates that the response to PUD hydrogel geometry is not common to all adherent cells, but it seems characteristic of endothelial cells.

Other factors, such as the degree of cross-linking in the hydrogel and the elastic modulus were evaluated. In the case of PUD hydrogels, the swelling property is related to the cross-linking ratio and to the ionic strength of the hydrating solutions (Fig. 3). As the feeding ratio of STMP increases, cross-linking density increases reducing swelling capacity [4]. Similarly, the presence of ions limited hydrogel expansion. An increase in cross-linking also caused an increase of the elastic modulus (from 300 Pa to 3 kPa), but this did not affect endothelial cell adhesion.

In the case of PUD hydrogels with large channels, cells in the channel started to adhere after at least 7 days and in a low number; cell aggregates and individual adhered cells cohabitated at that moment (Fig. 5A). This late adhesion was likely mediated by the deposition of ECM on hydrogel by the cells. In agreement with this hypothesis, it was possible to promote early adhesion of the cells in large channels by simply impregnating the hydrogels with collagen type I (2 mg/mL) during 4 h prior to cell seeding (Fig. S4). In this case, cell adhesion occurred within the first hours after cell seeding.

Taking these results into account, an explanation for the different adhesion observed as a function of the curvature, would be related to differences in the secretion of proteins from the ECM by the cells. The fact that the cells are not able to adhere to the surface of the hydrogels, as shown in Fig. 4A, proves the absence of motifs of adhesion in the biomaterial. In the case of the adhesion observed in the smaller diameter channels, the adhesion could be attributed to a cell confinement effect, a microfluidic effect or a higher concentration of serum proteins in the culture medium. However, the absence of adhesion in channels of the same size in hydrogels of another polysaccharide, such as agarose, rules out these hypotheses. The fact of observing a cellular adhesion in hydrogels coated with ECM proteins such as collagen, regardless of the diameter of the channel, as well as a delayed adhesion in the case of larger diameter channels, suggests that the cells could respond to curvature secreting proteins from the ECM early in the smaller diameter channels. The detection of laminin in Fig. 7C is consistent with this hypothesis.

Cell alignment has been described on cultured endothelial cells under flow conditions, and endothelial cells in the organism are exposed to a shear stress caused by the blood flow that induces cell alignment [43]. Here, this alignment was observed under static cell culture conditions and it must be noticed that it was not observed in hydrogels with large channels impregnated with collagen.

The three endothelial cell phenotypes characteristic of the sprouting angiogenesis, namely tip cells, stalk cells and quiescent cells coexisted in the small caliber channels [44]. In animal and human tissues, vessels are constituted of quiescent endothelial cells with poor regenerative activity in physiological conditions, except during embryo development, wound healing and in response to ovulation. Following a hypoxic stimulus, a cell is selected to lead vessel enlargement. This tip cell is characterized by a phenotype with extension of lamellipodia and filopodia to migrate towards the angiogenic stimulus [9,44,45]. Stalk cells are located between the quiescent cells and the tip cell; they divide and establish the vessel lumen. In the micro-channels formed here within the hydrogel, cells with the phenotype of tip cells were clearly observed after 48–72 h (Fig. 6). These cells presented invasive and motile behavior. In contrast to quiescent-like cells that formed a monolayer on the bottom of the channel, polarized cells were located mainly on the sides and upper surface of the channels and ended to form a cell network throughout time (see 96 h bottom and top in Fig. 6). This indicates that cells tended to migrate through the whole channel and were able to move against gravity forces even if they were not able to fully proliferate on top of the channel to form a complete cell layer to cover the channel. Nevertheless, after turning the hydrogel cells migrated and coated the whole channel. Based on this, a simple cell culture protocol was established to obtain fully endothelialized channels of 5 mm length within the polysaccharide hydrogel.

5. Conclusion

In this study, polysaccharide-based hydrogels made of neutral pullulan and dextran (PUD) that do not allow cell adhesion, were transformed into active materials guiding cell behavior by modification of the internal microarchitecture. The fabrication of tubular constructs with a particular curvature induced endothelial cell adhesion, migration, proliferation and polarization inside the channels (Fig. 8), indicating that cells are sensitive to the curvature of the channels and responded by secreting ECM that allowed cells to specifically adhere and organize in tubes.

Further development of the material will serve to improve the knowledge about the cellular response to the curvature of the seeding substrate and to better understand the mechanotransduction of geometrical cues. From a tissue engineering point of view, this material opens new perspectives to promote the vascularization of hydrogels. In a recent publication, we show the interest of pullulan and dextran hydrogels for the culture of liver cell spheroids in the pores of the biomaterial [5]. Experiments to co-culture endothelial cells in the channels with other type of cells, such as hepatic cells in organoids, in the pores of the hydrogels, are undergoing for this purpose. The strategy to form channels in the hydrogel is currently being adapted to form more complex vascular-like networks.

CRediT authorship contribution statement

Teresa Simon-Yarza: Conceptualization, Methodology, Investigation, Writing – Original Draft, Visualization **Marie-Noëlle Labour**: Conceptualization, Investigation **Rachida Aid-Launais**: Investigation **Didier Letourneur**: Writing – Review and Editing, Supervision, Funding acquisition.

Declaration of competing interest

The authors declare that they have no known competing financial interests or personal relationships that could have appeared to influence the work reported in this paper.

Acknowledgements

This work was support by Inserm, Université de Paris and Université Sorbonne Paris Nord. M-N. L. postdoctoral fellowship was supported by RHU iLite (grant number ANR-16-RHUS-0005). The authors greatly acknowledge Samira Benadda of the CRI U1149 Imaging Facility. Jean-Noël Rey is also acknowledge for his kind help with the 3D printing.

Appendix A. Supplementary data

Supplementary data to this article can be found online at https://doi.org/10.1016/j.msec.2020.111369.

References

[1] M.P. Lutolf, J.A. Hubbell, Synthetic biomaterials as instructive extracellular microenvironments for morphogenesis in tissue engineering, Nat. Biotechnol. 23 (2005) 47–55, https://doi.org/10.1038/nbt1055.
[2] R. Langer, D.A. Tirrell, Designing materials for biology and medicine, Nature. 428 (2004) 487–492, https://doi.org/10.1038/nature02388.
[3] E. Caló, V.V. Khutoryanskiy, Biomedical applications of hydrogels: a review of patents and commercial products, Eur. Polym. J. 65 (2015) 252–267, https://doi.org/10.1016/J.EURPOLYMJ.2014.11.024.
[4] J. Grenier, H. Duval, F. Barou, P. Lv, B. David, D. Letourneur, Mechanisms of pore formation in hydrogel scaffolds textured by freeze-drying, Acta Biomater. 94 (2019) 195–203, https://doi.org/10.1016/j.actbio.2019.05.070.
[5] M.-N. Labour, C. Le Guilcher, R. Aid-Launais, N. Samad, S. Lanouar, T. Simón-Yarza, D. Letourneur, Development of 3D hepatic constructs within polysaccharide-based scaffolds with tunable properties, Int. J. Mol. Sci. 21 (2020) 3644.
[6] S. Lanouar, R. Aid-Launais, A. Oliveira, L. Bidault, B. Closs, M.-N. Labour, D. Letourneur, Effect of cross-linking on the physicochemical and in vitro properties of pullulan/dextran microbeads, J. Mater. Sci. Mater. Med. 29 (2018) 77, https://doi.org/10.1007/s10856-018-6085-x.
[7] Y. Zheng, M.A. Roberts, Tissue engineering: scalable vascularized implants, Nat. Mater. 15 (2016) 597–599, https://doi.org/10.1038/nmat4637.
[8] G. Forgacs, Perfusable vascular networks, Nat. Mater. 11 (2012) 746–747, https://doi.org/10.1038/nmat3412.
[9] T. Simón-Yarza, F.R. Formiga, E. Tamayo, B. Pelacho, F. Prosper, M.J. Blanco-Prieto, Vascular endothelial growth factor-delivery systems for cardiac repair: an overview, Theranostics. 2 (2012) 541–552, https://doi.org/10.7150/thno.3682.
[10] S. van Helvert, C. Storm, P. Friedl, Mechanoreciprocity in cell migration, Nat. Cell Biol. 20 (2018) 8–20, https://doi.org/10.1038/s41556-017-0012-0.
[11] L.A. Rocha, R.A. Sousa, D.A. Learmonth, A.J. Salgado, The role of biomaterials as angiogenic modulators of spinal cord injury: mimetics of the spinal cord, cell and angiogenic factor delivery agents, Front. Pharmacol. 9 (2018) 164, https://doi.org/10.3389/fphar.2018.00164.
[12] D.G. Belair, M.J. Miller, S. Wang, S.R. Darjatmoko, B.Y.K. Binder, N. Sheibani, W.L. Murphy, Differential regulation of angiogenesis using degradable VEGF-binding microspheres, Biomaterials. 93 (2016) 27–37, https://doi.org/10.1016/j.biomaterials.2016.03.021.
[13] N. Yin, Y. Han, H. Xu, Y. Gao, T. Yi, J. Yao, L. Dong, D. Cheng, Z. Chen, VEGF-conjugated alginate hydrogel prompt angiogenesis and improve pancreatic islet engraftment and function in type 1 diabetes, Mater. Sci. Eng. C 59 (2016) 958–964, https://doi.org/10.1016/j.msec.2015.11.009.
[14] L.R. Nih, S. Gojgini, S.T. Carmichael, T. Segura, Dual-function injectable angiogenic biomaterial for the repair of brain tissue following stroke, Nat. Mater. 17 (2018) 642–651, https://doi.org/10.1038/s41563-018-0083-8.
[15] M. Zhu, W. Li, X. Dong, X. Yuan, A.C. Midgley, H. Chang, Y. Wang, H. Wang, K. Wang, P.X. Ma, H. Wang, D. Kong, In vivo engineered extracellular matrix scaffolds with instructive niches for oriented tissue regeneration, Nat. Commun. 10 (2019), https://doi.org/10.1038/s41467-019-12545-3.
[16] R.M. Linville, N.F. Boland, G. Covarrubias, G.M. Price, J. Tien, Physical and chemical signals that promote vascularization of capillary-scale channels, Cell. Mol. Bioeng. 9 (2016) 73–84, https://doi.org/10.1007/s12195-016-0429-8.
[17] J.S. Choi, Y. Piao, T.S. Seo, Fabrication of a circular PDMS microchannel for constructing a three-dimensional endothelial cell layer, Bioprocess Biosyst. Eng. 36 (2013) 1871–1878, https://doi.org/10.1007/s00449-013-0961-z.
[18] R. Vecchione, G. Pitingolo, D. Guarnieri, A.P. Falanga, P.A. Netti, From square to circular polymeric microchannels by spin coating technology: a low cost platform for endothelial cell culture, Biofabrication. 8 (2016) 025005, , https://doi.org/10.1088/1758-5090/8/2/025005.
[19] J.S. Miller, K.R. Stevens, M.T. Yang, B.M. Baker, D.-H.T. Nguyen, D.M. Cohen, E. Toro, A.A. Chen, P.A. Galie, X. Yu, R. Chaturvedi, S.N. Bhatia, C.S. Chen, Rapid

casting of patterned vascular networks for perfusable engineered three-dimensional tissues, Nat. Mater. 11 (2012) 768–774, https://doi.org/10.1038/nmat3357.
[20] A.C. Daly, P. Pitacco, J. Nulty, G.M. Cunniffe, D.J. Kelly, 3D printed microchannel networks to direct vascularisation during endochondral bone repair, Biomaterials. 162 (2018) 34–46, https://doi.org/10.1016/j.biomaterials.2018.01.057.
[21] R. Xie, W. Zheng, L. Guan, Y. Ai, Q. Liang, Engineering of hydrogel materials with perfusable microchannels for building vascularized tissues, Small. (2019), https://doi.org/10.1002/smll.201902838 1902838.
[22] C.K. Arakawa, B.A. Badeau, Y. Zheng, C.A. DeForest, Multicellular vascularized engineered tissues through user-programmable biomaterial photodegradation, Adv. Mater. 29 (2017), https://doi.org/10.1002/adma.201703156 1703156.
[23] N. Brandenberg, M.P. Lutolf, In situ patterning of microfluidic networks in 3D cell-laden hydrogels, Adv. Mater. 28 (2016) 7450–7456, https://doi.org/10.1002/adma.201601099.
[24] M. Werner, S.B.G. Blanquer, S.P. Haimi, G. Korus, J.W.C. Dunlop, G.N. Duda, D.W. Grijpma, A. Petersen, Surface curvature differentially regulates stem cell migration and differentiation via altered attachment morphology and nuclear deformation, Adv. Sci. 4 (2017) 1600347, https://doi.org/10.1002/advs.201600347.
[25] S. Oh, K.S. Brammer, Y.S.J. Li, D. Teng, A.J. Engler, S. Chien, S. Jin, Stem cell fate dictated solely by altered nanotube dimension, Proc. Natl. Acad. Sci. U. S. A. 106 (2009) 2130–2135 http://www.pnas.org/content/106/7/2130.full.pdf , Accessed date: 23 October 2017.
[26] J.Y. Park, D.H. Lee, E.J. Lee, S.H. Lee, Study of cellular behaviors on concave and convex microstructures fabricated from elastic PDMS membranes, Lab Chip 9 (2009) 2043–2049, https://doi.org/10.1039/b820955c.
[27] R.M. Gouveia, E. Koudouna, J. Jester, F. Figueiredo, C.J. Connon, Template curvature influences cell alignment to create improved human corneal tissue equivalents, Adv. Biosyst. 1 (2017) 1700135, https://doi.org/10.1002/adbi.201700135.
[28] N. Jain, K.V. Iyer, A. Kumar, G.V. Shivashankar, Cell geometric constraints induce modular gene-expression patterns via redistribution of HDAC3 regulated by actomyosin contractility, Proc. Natl. Acad. Sci. U. S. A. 110 (2013) 11349–11354, https://doi.org/10.1073/pnas.1300801110.
[29] V. Malheiro, F. Lehner, V. Dinca, P. Hoffmann, K. Maniura-Weber, Convex and concave micro-structured silicone controls the shape, but not the polarization state of human macrophages, 4 (2016) 1527–1706, https://doi.org/10.1039/c6bm00425c.
[30] M. Rumpler, A. Woesz, J.W.C. Dunlop, J.T. Van Dongen, P. Fratzl, The effect of geometry on three-dimensional tissue growth, J. R. Soc. Interface 5 (2008) 1173–1180, https://doi.org/10.1098/rsif.2008.0064.
[31] S.A. Ruiz, C.S. Chen, Emergence of patterned stem cell differentiation within multicellular structures, Stem Cells 26 (2008) 2921–2927, https://doi.org/10.1634/stemcells.2008-0432.
[32] K.A. Kilian, B. Bugarija, B.T. Lahn, M. Mrksich, L.L. Kiessling, Geometric cues for directing the differentiation of mesenchymal stem cells, Proc. Natl. Acad. Sci. U. S. A. 107 (2010) 4872–4877, https://doi.org/10.1073/pnas.0903269107.
[33] M.-H. Kim, Y. Sawada, M. Taya, M. Kino-Oka, Influence of surface topography on the human epithelial cell response to micropatterned substrates with convex and concave architectures, J. Biol. Eng. 8 (2014) 1–9, https://doi.org/10.1186/1754-1611-8-13.
[34] Q. Li, A. Kumar, E. Makhija, G.V. Shivashankar, The regulation of dynamic mechanical coupling between actin cytoskeleton and nucleus by matrix geometry, Biomaterials 35 (2014) 961–969, https://doi.org/10.1016/j.biomaterials.2013.10.037.
[35] G. Mocanu, D. Mihai, D. Le Cerf, L. Picton, G. Muller, Synthesis of new associative gel microspheres from carboxymethyl pullulan and their interactions with lysozyme, Eur. Polym. J. 40 (2004) 283–289.
[36] V. Dulong, R. Forbice, E. Condamine, D. Le Cerf, L. Picton, Pullulan–STMP hydrogels: a way to correlate crosslinking mechanism, structure and physicochemical properties, Polym. Bull. 67 (2011) 455–466, https://doi.org/10.1007/s00289-010-0435-2.
[37] A. Autissier, C. Le Visage, C. Pouzet, F. Chaubet, D. Letourneur, Fabrication of porous polysaccharide-based scaffolds using a combined freeze-drying/cross-linking process, Acta Biomater. 6 (2010) 3640–3648, https://doi.org/10.1016/j.actbio.2010.03.004.
[38] A. Purnama, R. Aid-Launais, O. Haddad, M. Maire, D. Mantovani, D. Letourneur, H. Hlawaty, C. Le Visage, Fucoidan in a 3D scaffold interacts with vascular endothelial growth factor and promotes neovascularization in mice, Drug Deliv. Transl. Res. 5 (2015) 187–197, https://doi.org/10.1007/s13346-013-0177-4.
[39] A. Pietrzyk-Nivau, S. Poirault-Chassac, S. Gandrille, S.-M. Derkaoui, A. Kauskot, D. Letourneur, C. Le Visage, D. Baruch, Three-dimensional environment sustains hematopoietic stem cell differentiation into platelet-producing megakaryocytes, PLoS One 10 (2015) e0136652, , https://doi.org/10.1371/journal.pone.0136652.
[40] I. Matai, G. Kaur, A. Seyedsalehi, A. McClinton, C.T. Laurencin, Progress in 3D bioprinting technology for tissue/organ regenerative engineering, Biomaterials 226 (2020), https://doi.org/10.1016/j.biomaterials.2019.119536.
[41] J. Nie, Q. Gao, Y. Wang, J. Zeng, H. Zhao, Y. Sun, J. Shen, H. Ramezani, Z. Fu, Z. Liu, M. Xiang, J. Fu, P. Zhao, W. Chen, Y. He, Vessel-on-a-chip with hydrogel-based microfluidics, Small. 14 (2018) 1–14, https://doi.org/10.1002/smll.201802368.
[42] J. Nie, Q. Gao, C. Xie, S. Lv, J. Qiu, Y. Liu, M. Guo, R. Guo, J. Fu, Y. He, Construction of multi-scale vascular chips and modelling of the interaction between tumours and blood vessels, Mater. Horizons. 7 (2020) 82–92, https://doi.org/10.1039/c9mh01283d.
[43] R. Sinha, S. Le Gac, N. Verdonschot, A. van den Berg, B. Koopman, J. Rouwkema, Endothelial cell alignment as a result of anisotropic strain and flow induced shear stress combinations, Sci. Rep. 6 (2016) 29510, https://doi.org/10.1038/srep29510.
[44] P. Carmeliet, Angiogenesis in health and disease, Nat. Med. 9 (2003) 653–660, https://doi.org/10.1038/nm0603-653.
[45] R.H. Adams, K. Alitalo, Molecular regulation of angiogenesis and lymphangiogenesis, Nat. Rev. Mol. Cell Biol. 8 (2007) 464–478, https://doi.org/10.1038/nrm2183.